
Applied Moisture Engineering

Achilles N. Karagiozis, Ph.D.

Member ASHRAE

ABSTRACT

Many recent, moisture-related failures of wood frame construction in low-rise residential buildings and steel frame construction in high-rise residential/commercial buildings have created significant pressure to change construction codes in both Canada and the United States. However, solutions to moisture-induced problems may be difficult when several interacting mechanisms of moisture transport are present. A new approach to building envelope durability assessment has been introduced in North America, which employs experiments and advanced modeling to predict the long-term performances of building envelope systems. This permits the comparison and ranking of wall systems with respect to total hygrothermal performance. Elaborate experiments to measure the various hygrothermal properties, such as sorption and suction isotherms, vapor permeabilities, liquid diffusivities, and drainage, are combined with full-scale laboratory building envelope testing to determine system and subsystem performances, which are then included in the modeling activity to predict the long-term performances of building envelopes. This approach has been termed "moisture engineering."

This paper presents detailed results of an application of moisture engineering in North Carolina, where within the first six months of occupancy, some problems were observed in 3200 homes (Nisson 1995). All the homes employed an exterior insulation finish system (EIFS). An extensive laboratory and material testing analysis to determine the cause of failure was undertaken. A state-of-the-art transient two-dimensional and three-dimensional finite difference model was employed to numerically solve the heat, air, and moisture transport through various EIFS walls. The drying potential of each system was then numerically analyzed using real weather conditions, and results clearly demonstrated the limited drying potential for the wall system in that climate. From these results, moisture control strategies are identified.

INTRODUCTION

Exterior insulation finish wall systems have become one of the popular exterior building envelope systems in the residential and commercial construction market in North America. Essentially, these wall systems are based on the face sealed principle and consist of base and finish coats, a plastic foam insulation, a sheathing board (usually oriented strand board), OSB, plywood or gypsum board, an insulated cavity, a vapor retarder, and finally an interior gypsum board (see Figure 1). The advantage of these wall systems is that they are aesthetically pleasing, energy efficient, lightweight, and are a low construction cost wall cladding system. Surveys show that the exterior facade may be the most important standard by which the owner and public measure the quality of a building. Market potential for these systems is very favorable, both in

the energy retrofit applications as well as new constructions. Currently, the market share for residential buildings is approximately (260,000) 3% to 4% of exterior cladding systems in the U.S. market but increasing at a rate of 8% to 11% each year. In the U.S., the exterior insulation finish system (EIFS) siding on commercial construction accounts for 17% of the market (EIMA 1997).

EIFS walls were originally developed in northern Europe, where they have successfully been performing for the past 40 years. All these walls were designed based on the face seal approach. The methods, materials, and sheathing systems employed in Europe are, however, somewhat different from those employed in North America. EIFS in Europe are primarily applied to low-rise masonry or concrete substrata, which explains the differences found in the durability and performance of these walls. In Canada, EIFS were introduced in the

Achilles N. Karagiozis was a research officer at the National Research Council Canada, Ottawa, Ontario, when this work was conducted. He is now a senior research engineer at Oak Ridge National Laboratory, Oak Ridge, Tenn.

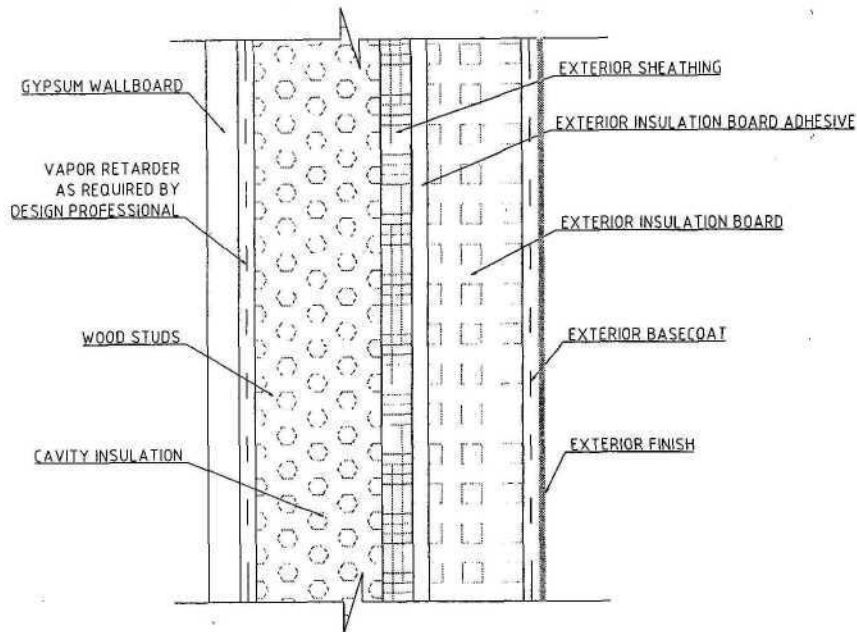


Figure 1 Face sealed EIFS wall.

late 1960s, and many applications are on high-rise buildings with gypsum-sheathed metal stud walls. Similarly in the United States, EIFS walls have been applied to high-rise commercial buildings but have found their way to residential low-rise buildings. EIFS wood frame construction, with oriented strand board as the exterior sheathing layer, is used extensively in the U.S.

Recently, Nisson (1995) presented a summary of the serious moisture problems in EIFS construction in the New Hanover County area of North Carolina, an area that is characterized by warm and humid conditions. Moisture problems ranging from high moisture content in the exterior sheathing to total rotting were uncovered. Apparently, nearly all of the 3200 EIFS homes needed some remedial measures. Since then, various studies and investigations by consultants and research organizations (Brown et al. 1997; Crandell and Kenny 1995), as well as EIFS manufacturers, have shed light on the causes of these failures. Most of the failures have been traced to flashing details and the penetration of water into the wall systems (Nelson and Waltz 1996). However, while water entry should be avoided for any building envelope system, an often overlooked fact is that these wall systems did not provide vapor and water management for drying of the enclosure.

The Canadian experience of EIFS walls in the climatic conditions of Vancouver, the Rocky Mountains, Calgary, Edmonton, and Toronto has been described in detail by Posey and Vlooswyk (1996). Twenty-five buildings that had been in service for two to thirteen years, new or retrofitted, were evaluated for field performance. Results showed that the exterior finish was in excellent condition in many cases, including the oldest building, which was a residential high-rise building. More than half of the installations were in good to excellent overall condition, although none were entirely free of defect.

According to Posey and Vlooswyk (1996), approximately 30% had visible problems serious enough to threaten service life if left uncorrected. Problems were summarized as failed joints, cracking, impact damage, excessively thin applications of finish and base coat, softening, erosion of color, delamination, poor attachment, fading, freezing during construction prior to curing, cracking at locations of movement in underlying supports, unsatisfactory repairs, algae and moss growth, water-saturated insulation damage from interior and exterior water sources, and complete detachment of the system from the building. Within this extensive field assessment, it was found that problems often seemed to appear when the system is substituted at the last moment for some other finish. If the exterior surface that is directly exposed to the environment is imperfect, there is no second line of defense, as all of these walls were based on the face-seal approach.

There has been a degree of condemnation of face-sealed wall systems. Such a statement cannot be made unconditionally since some standard face-seal EIFS constructions have performed satisfactorily in the past. Indeed, numerous investigations have shown that with proper design and quality control (workmanship), these systems can perform satisfactorily over extended periods of 10 to 15 years (Zwayer 1996). In a study titled "EIFS: When It Works and When It Does Not," Zwayer concludes that all problems that are present in EIFS can be avoided through proper attention to design, detailing, and installation of the material by the architects, manufacturer's representatives, manufacturers, and applicators. Essentially, problems occur as failures to leave proper space for the sealant joint, to properly back wrap panel edges, install the insulation, or to install expansion joints at proper locations. When proper attention and maintenance are provided, then EIFS is a successful option. On the other hand, there are some

environmental conditions in which the requirement for drainable systems is fully justified. The issue is, therefore, not acceptance or condemnation but a better understanding of the environmental conditions in which each of the systems is appropriate.

To date (July 1998), knowledge of the hygrothermal performance of EIFS walls that includes all climatic effects, such as rainwater penetration, solar radiation, night sky radiation, as well as the influence of wind speed and site/wall orientation on both the convective and mass transfer coefficients, is not available. This results in the misinterpretation of some of the hygrothermal processes that occur in these wall systems, which may limit the application of innovative strategies (such as materials with strong functional dependencies on transmission coefficients) that could potentially enhance the durability performance (Bomberg et al. 1997) of the wall systems.

In this work, the author presents a study conducted to determine the drying potential of a particular EIFS system by employing an integrated modeling and laboratory method. Work was conducted to provide insight on one aspect of the EIFS wall moisture problem in North Carolina. Elaborate material property testing was also conducted to characterize the hygrothermal properties of various material layers. Experiments were conducted to determine the water leakage rates of various assemblies with and without the influence of defects (Ulett 1996). Whole wall (no windows) and wall-window interface effects were also studied experimentally. The effect of water leakage into the wall cavity (OSB and insulation layer) as a function of air pressure difference and rainwater intensity was assessed. Information that defined the subsystem performances of the EIFS walls as well as material properties was then integrated into a state-of-the-art hygrothermal model, LATENITE (Karagiozis 1997a; Salonvaara and Karagiozis 1994). The model was then used to predict the integrated wall hygrothermal performance using real weather conditions. Two separate issues were studied: the drying potential due to initial construction moisture in a solid EIFS wall and water penetration due to wind-driven rain in the presence of a window-wall assembly. The present study addressed some of the issues present in vapor diffusion control strategies of these wall systems. All simulations were conducted using south-facing wall systems. The drying rate potential of the complete wall system, a concept not as commonly employed in moisture engineering, was adopted and further investigated for the climatic conditions of Wilmington, N.C.

Drying Potential/Performance Concept

All wall systems are susceptible to vapor and liquid moisture accumulation. A wall can be characterized with respect to its specific drying capability. This property provides a specific identity to the wall, describing in some sense its maximum moisture load tolerance. The drying potential is a function of the specific material properties, installation methods, and interior and exterior climatic conditions. The drying potential is

directly related to the moisture tolerance for moisture load design purposes. In effect, the drying potential of a wall system should be considered as a critical design factor during decision making in the choice of a particular envelope design. Architects and building envelope engineers must have the drying potential ranking of various wall systems available to assist in the selection of viable envelope wall systems.

Material Property Characterization

Properties for most of the materials were developed and correlated into the form required by the model. The thicknesses and densities were taken from Table 1; the thermal resistances of the OSB and EIFS panel (expanded polystyrene coated with a base and finish coat) from Table 2; the water vapor permeances of materials other than EPS, EIFS panel, and OSB from Table 3; the water absorption coefficients of OSB and EIFS panel from Table 4; the wood stud, concrete, and gypsum diffusivity from Table 5; and, finally, the full OSB moisture diffusivity from Table 6.

In addition, hygrothermal properties for gypsum were taken from existing measurements and all other material properties from the Material Property Database (Karagiozis et al. 1994). The water vapor transmission characteristics of EIFS panel or lamina (includes finish and basecoat layers), extruded

TABLE 1
Thickness and Density of the Test Materials/Samples

Material/Sample	Thickness mm	Density kg/m ³
EPS	24.3	14.4
EIFS Panel	28.0	—
OSB	11.5	661
Wood	—	425
Base Coat	—	1734
Finish Coat	—	1459
Concrete		2200
Glass Fiber		50

TABLE 2
Thermal Characteristics of the Materials

Material	Thermal Resistance, m ² ·K/W [Thermal Conductivity, W/(m·K)]
EPS	0.034
EIFS Panel	0.659
OSB	0.126
Wood	0.106
Gypsum	0.270

TABLE 3
Water Vapor Permeance of Various Materials

Material	Thickness, mm	Density, kg/m ³	RH%	Water Vapor Permeance, kg/(Pa·s·m ²)
OSB	11.5	661	77	2.1×10 ⁻¹⁰
Wood	10.0	425	30	2.76×10 ⁻¹⁰
Gypsum	12.7	620	30	0.151×10 ⁻¹⁰
Concrete	10.0	2200	30	1.55×10 ⁻¹⁰

TABLE 4
Water Absorption Coefficient of Various Materials

Material	Thickness, mm	Density, kg/m ³	Absorption Coefficient, kg/(m ² ·s ^{1/2})
OSB - Along the Strands	—	661	0.032
OSB - Across the Strands	11.5	661	0.0054
Wood - Along the grain	—	553	0.0087
Base Coat	—	1734	0.00014
Finish Coat	—	1459	0.00032

TABLE 5
Liquid Diffusivity of Various Materials

Material	Thickness, mm	Density, kg/m ³	Liquid diffusivity at 98% RH, m ² /s
Wood	—	425	0.73E-09
Gypsum	12.7	620	0.16E-06
Concrete	—	220	0.11E-07

TABLE 6
A Set of Values for the Moisture Diffusivity of OSB Along the Strands

Moisture Concentration, g/cm ³	Diffusivity, m ² /s	Moisture Concentration, g/cm ³	Diffusivity, m ² /s
0.011	2.3E-10	0.201	5.6E-10
0.030	3.0E-10	0.249	6.7E-10
0.068	3.7E-10	0.300	8.7E-10
0.103	4.1E-10	0.359	1.5E-09
0.153	4.8E-10	0.398	4.3E-09

polystyrene (EPS), oriented strand board, and pine wood (Kumaran et al. 1989) were determined according to the modified ASTM E 96 Test Method for Water Vapor Transmission of Materials (Lackey et al. 1997). Four different sets of rela-

TABLE 7
Vapor Transmission Properties

Sample	Panel	EPS	Coating
Average RH, %	Vapor Permeance, kg/s·m ² ·Pa		
16	1.1E-10	1.5E-10	3.3E-10
27	1.1E-10	1.5E-10	4.1E-10
77	1.2E-10	1.6E-10	5.1E-10
91	1.7E-10	2.2E-10	7.6E-10

tive humidities were used as boundary conditions in order to determine the dependence of vapor transmission characteristics as a function of relative humidity. Results for the EPS, panel, and coats are given in Table 7.

The vapor permeability and liquid diffusivity of the OSB layers as a function of relative humidity and moisture content, respectively, are presented in Figure 2.

DESCRIPTION OF THE MODEL

LATENITE 1.2 is a state-of-the-art hygrothermal model developed by Karagiozis and Salonvaara. A detailed model description of the version 1.0 hygrothermal model is given by Hens and Janssens (1993) and Karagiozis (1993). Version 1.2 is described by Salonvaara and Karagiozis (1994) and version 1.3 by Karagiozis (1997a). A brief overview of the model is presented in this paper. The moisture transport potentials used in the model are moisture content and vapor pressure; for energy transport, temperature is used. The equations are developed on a Cartesian rectangular coordinate system, contain explicit and implicit time discretizations, and are spatially discretized using the control volume formulation. Approximate factorization and full solution procedures are incorporated into the model to solve the differential equation in delta form. The model was recently upgraded to include the porous airflow through insulation and cracks by solving a subset of the Navier Stokes equations—Darcy's equations.

The model includes the capability for handling internal heat and moisture sources, gravity-driven liquid moisture, and surface drainage capabilities. An important feature of the upgraded model is its extension from providing deterministic solutions to stochastic statistically based ones. The model employs nonlinear hygrothermal properties as found in nature. The porous media transport of moisture (vapor and liquid) through each material layer is considered strongly coupled to the material properties (i.e., the sorption-suction curves).

The corresponding moisture fluxes are decomposed for each phase and are treated separately. The moisture transfer equation, including liquid and vapor transfer, is

$$q_M = -\rho_0 D_w(u, T) \nabla u - \delta_p(u, T) \nabla P_v + v_a \rho_v + K(u) \rho_w \vec{g} \quad (1)$$

where

$$q_M = \text{mass flux, kg/m}^2\text{-s;}$$

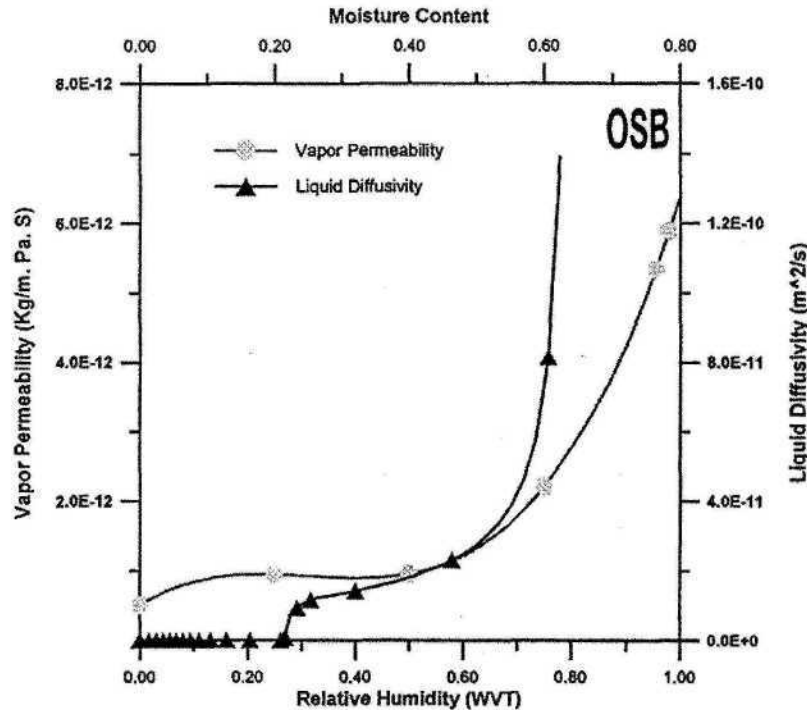


Figure 2 Water permeability and liquid diffusivity for OSB.

- ρ_0 = dry density of porous material, kg/m^3 ;
- D_w = liquid moisture diffusivity, m^2/s ;
- u = moisture content, kg_w/kg_d ;
- T = temperature, $^\circ\text{C}$;
- δ_p = vapor permeability, $\text{kg/s}\cdot\text{m}\cdot\text{Pa}$;
- P_v = vapor pressure, Pa ;
- v_a = velocity of air, m/s ;
- ρ_v = density of vapor in the air, kg/m^3 ;
- K = moisture permeability, s ;
- ρ_w = density of liquid water, kg/m^3 ;
- g = acceleration of free fall, m/s^2 .

Wind-Driven Rain

Wind-driven rain is a complex phenomenon itself, relatively unresearched and still not fully understood. Rain droplets with a wide range of sizes are transported by wind that has a distinct three-dimensional behavior near buildings. Rain droplet size distributions vary randomly with respect to time and space. For these reasons, the amount of rain striking the exterior surfaces of a building is unique to that building, as it depends on the local geometry of the building, topography around the building, wind speed, wind direction, rain intensity, and rain droplet distribution.

Knowledge available on wind-driven rain, albeit limited, has been predominately determined by field experiments (Lacy 1951, 1965; Schwarz and Schlagregen 1973). Recently, however, investigations employing computational fluid

dynamics (CFD) methods by Choi (1991,1992), Wisse (1994), and Karagiozis and Hadjisophocleous (1995) have appeared. Both experimental and numerical results show agreement on rain intensity factors. In Figure 3, typical rain trajectories are shown for a full range of rain droplet sizes; these results were obtained by Karagiozis et al. (1997) using a commercially available CFD model (ASC 1993). Correlations were then developed from many series of rain-droplet simulations that were included in the hygrothermal model. Wind-driven rain is modeled as a source term on the exterior wall surface. However, the amount of water that can penetrate into the porous material is limited by the maximum allowable moisture content in the exterior material. Figure 3 shows the rain droplet trajectories impinging on two buildings.

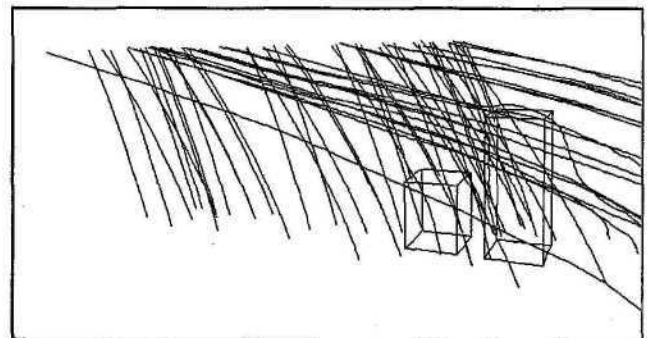


Figure 3 Rain trajectories on buildings.

PROBLEM DESCRIPTION

The hygrothermal performance of two EIFS walls are investigated in this paper. The wall systems are essentially of the same structure, but one includes a solid wall structure while the other includes the effects of water penetration at windows. These wall systems are defined throughout this paper as solid EIFS walls and the EIFS walls with a window.

These two wall systems, as shown in Figures 4 and 5, incorporated a solid concrete crawl space subsystem and all material layer details that could be described in a two-dimensional analysis. These are the wood joists, the plywood subfloor layer, the upper and bottom wood stud portions, sill plate, oriented strand board (OSB) sheathing, gypsum board,

extruded polystyrene (EPS), glass fiber insulation, base coat and finish coat, polyethylene sheet vapor retarder, and interior paints. Special effort was made to develop a computational model that was as close as possible to realistic geometrical conditions.

Solid EIFS Walls

For the solid EIFS wall, the drying potential of four wall assemblies was investigated (Table 8). Two different water vapor permeance interior paints representing poor and good quality gypsum board paint were employed in the study. The objectives of these simulations were to determine the effect of the polyethylene sheet vapor retarder and interior paint coat-

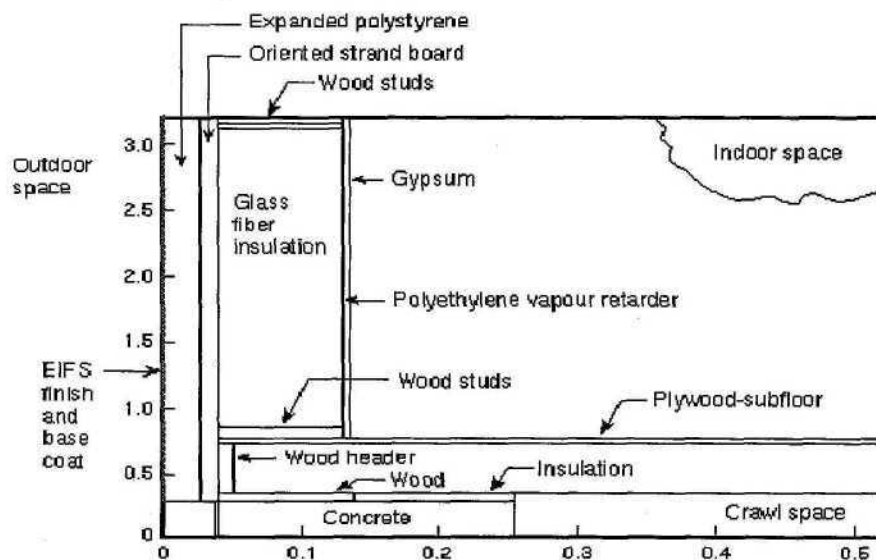


Figure 4 Solid EIFS wall (note different scales for x and y directions [m]).

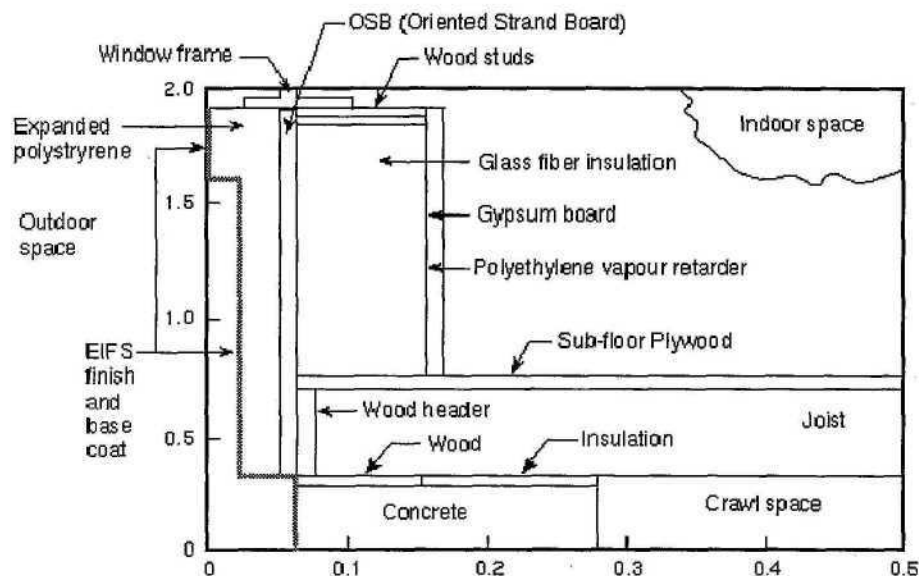


Figure 5 EIFS with window (note different scales for x and y scales [m]).

TABLE 8
Simulation Cases for EIFS Solid Wall System

Wall Designation	Interior Water Vapor Permeance		Window Water Leakage
	Polyethylene Film	Paint	
WALL1	Yes	No Paint	No Leak
WALL2	No	No Paint	No Leak
WALL3	No	High WVP Paint ¹	No Leak
WALL4	No	Low WVP Paint ²	No Leak

¹ Paint/gypsum board with high water vapor permeance of 210 ng/(Pa·s·m²).
² Paint/gypsum board with low water vapor permeance of 30 ng/(Pa·s·m²).

ings and to characterize the drying potential of the various wall assemblies. The OSB layer for these simulations was initially assigned rather wet moisture content conditions of 0.21 kg_w/kg_{dry}; this will be discussed further in the section on initial conditions.

EIFS Walls with Windows

Three EIFS wall cases were simulated with the presence of window defects (water penetration). The water leakage characteristics were determined by laboratory experiments carried out by Ullett (1996).

BOUNDARY AND INITIAL CONDITIONS

For this study, both the interior and exterior boundary conditions varied as a function of time of year. For the exterior

boundary conditions, three-year weather data were purchased from the Natural Resource Center of the National Climatic Data Center (NCDC 1995) for the city of Wilmington, North Carolina. Wilmington is on the mid-Atlantic seacoast where summer climatic conditions are hot and humid. The ASHRAE Handbook (ASHRAE 1997) lists the 2.5% summer design conditions as 33°C dry-bulb and 26°C coincident wet-bulb temperatures, which corresponds to a 58% design relative humidity. The 2.5% winter design temperature is -3°C. The purchased data were employed in the simulation of the hygro-thermal performance of the EIFS walls. Interior boundary condition data files were produced in which the temperature in the summer period varied from 23°C to 25°C and in the winter from 20°C to 23°C. The interior relative humidity was maintained constant at 55% RH during the summer periods and at 35% RH during the winter periods; these interior conditions were provided by USG (1996). The heat transfer coefficients for external and internal surfaces were kept constant at 25 and 10 W/(m²·K), respectively. The mass transfer coefficients are dependent on the values of the heat transfer coefficients (Lewis relations) and were assigned values of 7.4E-08 and 1.9E-07 kg/(m²·s·Pa) for the interior and exterior surfaces, respectively. The monthly average temperatures and vapor pressures and vapor pressure differences ($P_{exterior} - P_{interior}$) for Wilmington are shown in Figure 6. The yearly average temperature and vapor pressure in Wilmington is 16.5°C, and 1378 Pa, respectively. Hourly weather data were used as boundary conditions. The years represented are 1989, 1990, and 1991. They have been analyzed and compared with the weather data of 1995 and exhibit greater extremes with respect to the transient wind and rain behavior. In these weather files, the exterior temperature, relative humidity, solar radiation,

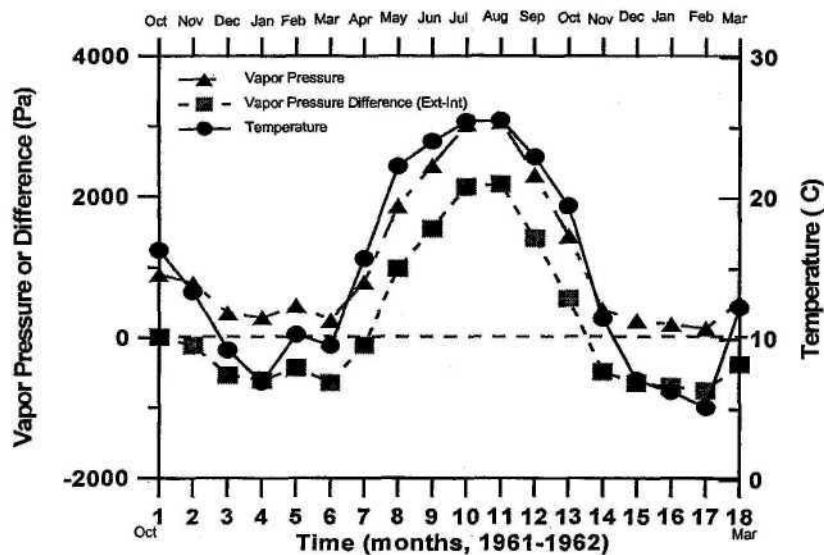


Figure 6 The monthly average temperatures, vapor pressures, and vapor pressure difference (exterior-interior) for Wilmington weather conditions for the period 1961-1962.

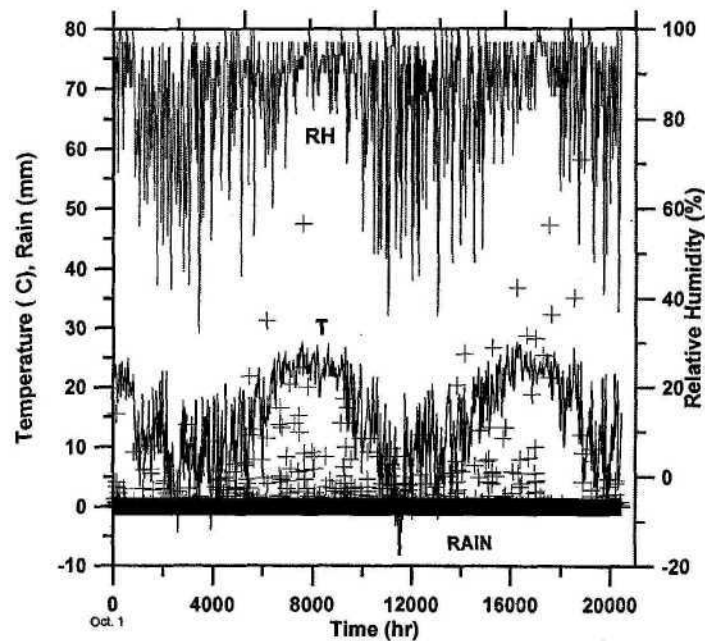


Figure 7 Weather data for the 2.5 year simulation period (Crosses (+) are employed as Symbols for Rain).

wind speed and direction, and rain precipitation were recorded and hourly data were extracted.

Solar radiation and longwave radiation from the outer surfaces of the wall were included in the analysis. The solar absorptance of the wall was assumed to be 0.6. Figure 7 shows the temperature, relative humidity, and rain data for the three-year period. The wall systems employed in this analysis were only assumed to be facing south.

The exterior surfaces were exposed to the amount of rain that hits a vertical wall. Additional simulations were performed to determine the runoff effect in the cases that included the window. Driving rain was used in the analysis as calculated by employing a commercially developed model (ASC 1993). An equation for wind-driven rain used in the hygrothermal model was based on a numerical study (Karagiozis and Hadjisophocleous 1995) that presents the results generated by the wind-driven rain droplet simulations. This information was then adjusted employing a correlation generated from measured quantities (Ullett 1996) and was implemented in the model as a defect (moisture source) for the simulation cases that included the effects of the window.

Solid EIFS Walls

Wet initial conditions were investigated in the solid EIFS wall simulation cases. The OSB sheathing was assigned an initial relative humidity (relative humidity in the pores of a material is related to moisture content via the sorption isotherm) of 98% (moisture content of $0.21 \text{ kg}_w/\text{kg}_{dry}$, while all other material layers were assigned a relative humidity of 80%. The initial moisture conditions represent situations where either water penetration has occurred or initial construction moisture is present. All layers were assigned an

initial temperature of 15°C . The simulations were carried out for a three-year exposure starting from the first of October. Details of the envelope system modeled for the solid EIFS walls are given in Figure 4.

EIFS Walls with Windows

The EIFS walls with windows (defect, with water penetration cases) were assumed initially wet by assigning relative humidity values for the wood and OSB layers of 98% (OSB moisture content of $0.21 \text{ kg}_w/\text{kg}_{dry}$). All remaining layers were assigned values of 80% RH. All layers were assigned an initial temperature of 15°C . Again, as for the solid EIFS wall systems, the simulations were carried out for a three-year period starting from the first of October. Details of the complete envelope system modeled for the EIFS walls with windows are given in Figure 5.

The measured water vapor permeabilities and liquid diffusivities for EIFS panel and oriented strand board and other materials that were employed in the simulations (Tables 3, 4, 5, 6, and 7).

The wall was exposed to outside air temperature and the relative humidity that varied according to the weather data from the selected location (Wilmington). In this study, no air infiltrating or exfiltrating was considered; therefore, the primary mode of water transmission is due to diffusion processes, both vapor and liquid transport.

SIMULATION ASSUMPTIONS

Two main assumptions were employed in the computer modeling of the hygrothermal performance of the EIFS walls:

- a. each material layer is homogeneous;

- b. water penetration characteristics of the EIFS walls are similar to those measured in the laboratory.

Simulation Results

For all simulations, the LATENITE 1.2 hygrothermal model was employed, and the deterministic solution method was invoked. Simulation results are presented for all cases. Seven wall cases were simulated, four examining the drying and net yearly moisture accumulation for the solid EIFS wall systems (WALL1, WALL2, WALL3, WALL4) or (Case1, Case2, Case3, Case4) and three examining the drying and net yearly moisture accumulation for the window defect cases with different water penetration characteristics (WALL5, WALL6, WALL7) or (Case5, Case6, Case7). The terms "WALL" and "Case" represent the same system and are used interchangeably.

Solid EIFS Walls

The time-related changes of mean moisture content per meter of wall width are presented in Figures 8-10. In Figure 8, the total amount of moisture present in the wall system as a function of time is presented to show the relative hygrothermal performance of the EIFS wall for the four different vapor control strategies. The simulations start from the first day of October (1989) for a period of three years; however, in this figure, only two months of data are shown. As these walls represent solid EIFS walls, only drying is observed. The wall with the polyethylene vapor retarder dried the slowest (WALL1 or Case1), followed by the wall without a vapor retarder but with a paint coating of $30 \text{ ng}/(\text{Pa}\cdot\text{s}\cdot\text{m}^2)$ (WALL4 or Case4), then the wall without a vapor retarder but with a paint coating of $210 \text{ ng}/(\text{Pa}\cdot\text{s}\cdot\text{m}^2)$ (WALL3). The fastest drying was observed for the wall without a vapor retarder and with no paint (WALL2). From this figure it becomes apparent that the preferred drying of this wall system in Wilmington is primarily toward the interior. Indeed, for higher inside relative

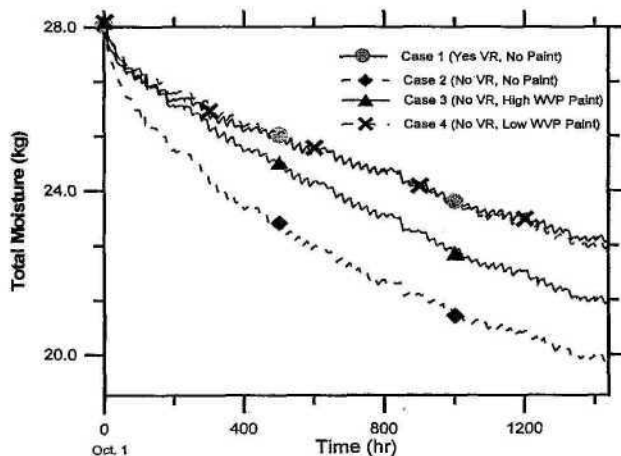


Figure 8 Transient total wall moisture distribution for the first two months (X-scale is hours).

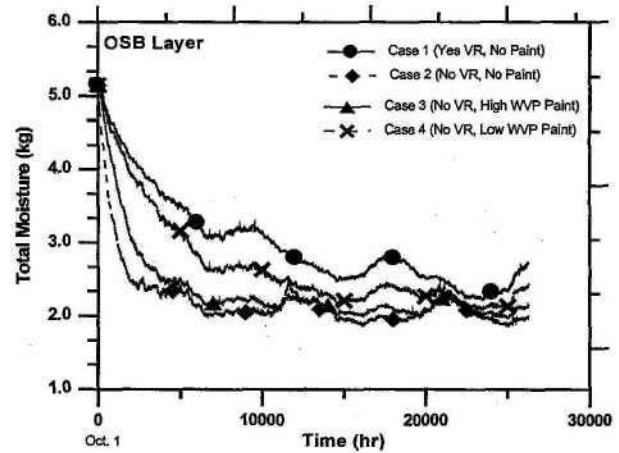


Figure 9 Transient moisture distribution in OSB layer.

humidity, the drying potential of the overall wall system will be substantially reduced. WALL2 and WALL3 reach steady dry conditions within the first six months, while the other two walls with the vapor retarder and low permeance paint take several years.

Figure 9 shows the transient moisture content trend as a function of time for the oriented strand board (OSB) sheathing layer. The X-axis represents the full three-year simulation period. This material layer is one of the most critical layers in terms of durability and potential for mold growth. Rapid drying is observed for the no-retarder case, followed by the wall without a vapor retarder but with a paint coating of $210 \text{ ng}/(\text{Pa}\cdot\text{s}\cdot\text{m}^2)$ (WALL3), then the wall without a vapor retarder but with a paint coating of $30 \text{ ng}/(\text{Pa}\cdot\text{s}\cdot\text{m}^2)$ (WALL3), and, finally, the slowest drying was observed by the wall that included the 6-mil polyethylene (WALL1).

Figure 10 depicts the moisture behavior for the glass-fiber insulation layer. Similar drying trends are observed as

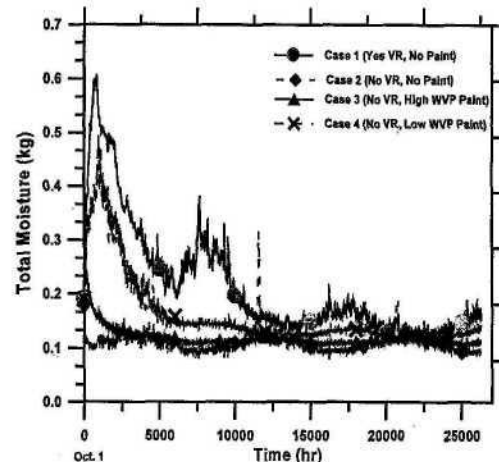


Figure 10 Transient moisture distribution in fiberglass layer

those for the OSB layer; higher moisture contents are also present in the walls that have tighter vapor control.

Figures 11, 12, and 13 show the transient RH distributions within the OSB layer at three different heights corresponding to 0.1, 1.1, and 2.2 meters from ground level for WALL1 and WALL2. These two wall systems correspond to the walls with the highest and lowest interior vapor control. Three points within the horizontal cross section of the OSB board are plotted out. It becomes evident that natural convection develops a two-dimensional moisture distribution that results in uneven moisture contents within the OSB layer. The top of the OSB layer is exposed to higher moisture content levels than the middle location. The bottom also displays higher moisture contents than the middle layers. Indeed, this coincides with field observations that the upper and bottom levels of the OSB layer tend to rot rather than the middle height locations. In these figures, a line is drawn to show potential danger levels of relative humidities that could cause mold fungi development. This line corresponds to a conservative mold deterrent

level of 70% RH. Employing this performance criterion set point, it is evident that the middle height OSB region dries out within 20 days for WALL2 while it takes close to 900 days in the top region for WALL1.

Figure 14 summarizes the relative drying performance of all four wall systems giving the time for each wall to reach an average 70% RH in the OSB. The drying multiplication factor is defined as how many times faster the walls dry out with respect to WALL2. It is observed that WALL1 dries 25 times slower to the mean 70% RH than WALL2. This figure summarizes the effect of interior vapor control strategies on the drying performance of a solid EIFS wall in the specific location of Wilmington.

EIFS Wall Systems with Windows

Figure 15 shows the transient moisture content OSB distributions for WALL5, WALL6, and WALL7. Here the effect of the window defect is clearly depicted. As the water penetration rate becomes higher, a net yearly moisture accu-

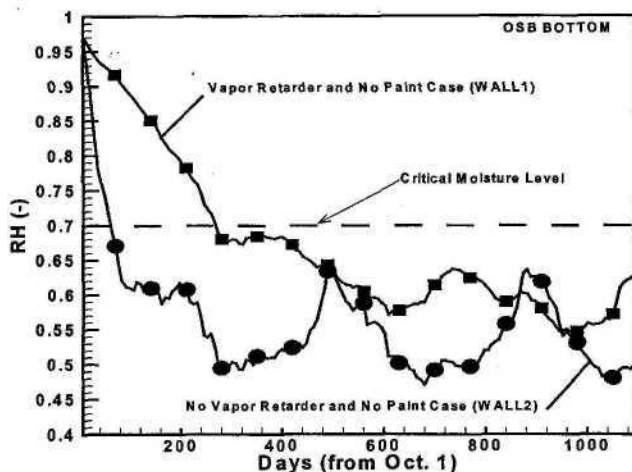


Figure 11 Spatial and transient relative humidity distribution in OSB (Bottom).

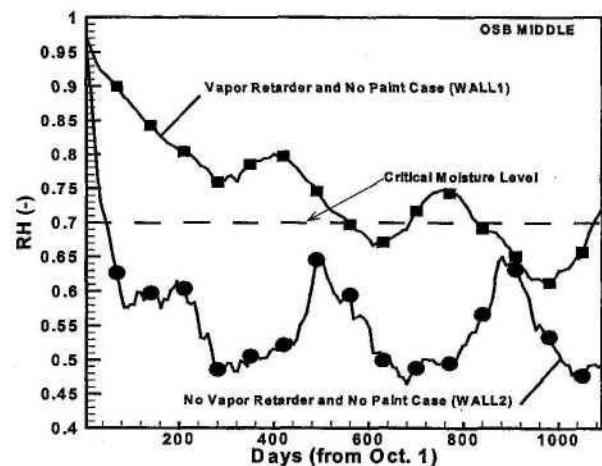


Figure 12 Spatial and transient relative humidity distribution in OSB (Middle).

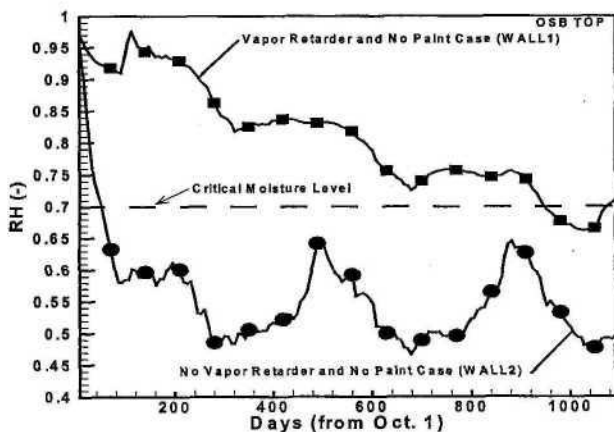


Figure 13 Spatial and transient relative humidity distribution in OSB (Top)

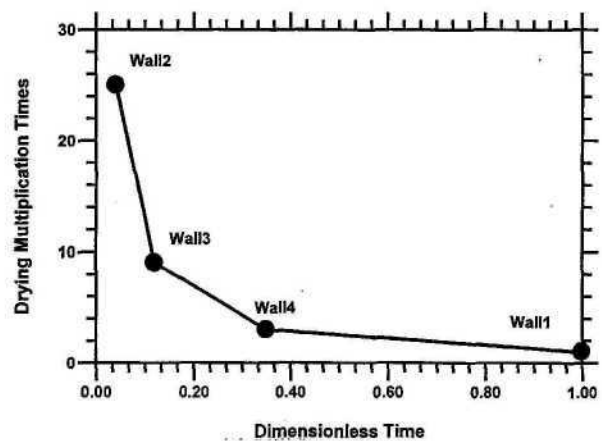


Figure 14 Drying performance of EIFS solid wall.

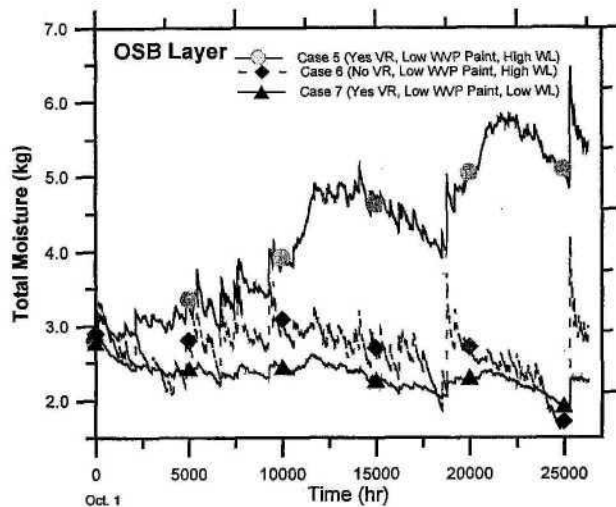


Figure 15 Transient total moisture in window/wall

mulation is observed for the case with a vapor retarder (WALL5). For the case without a vapor retarder, moisture can dry inward, even for a wall with high water penetration rate (WALL6), but high localized moisture content conditions still exist under windows. In the simulation cases with low water penetration rates (WALL7), the wall could dry out even with the vapor retarder, but, again, high moisture contents are present. For WALL5, six kilograms of moisture accumulated within the wall assembly. In the OSB layer alone, the moisture accumulated at a rate of 1 kg per year, and additional moisture accumulation occurred in the insulation layer.

CONCLUSIONS

Vapor diffusion control strategies have a significant effect on the hygrothermal performance (drying potential) of EIFS walls for mixed climatic conditions. This study, which included the effects of vapor transport, liquid transport, and natural convection effects, found that the use of a polyethylene vapor retarder (type I or type II) may not be beneficial to drying the initial construction moisture. The results showed slow drying even for the no-retarder case, as the drying potential for climatic conditions of Wilmington are not very favorable.

Results generated from the simulation characterized the drying capabilities of various interior vapor control strategies. These were carried out for climatic conditions found in Wilmington, North Carolina. Results show the significant influence of interior vapor control on the drying potential of EIFS wall systems, making questionable the strict use of 6-mil polyethylene vapor retarder in EIFS wall systems in that climatic zone. The wall systems investigated were not by any means optimized as far as vapor and liquid control is concerned. The effect of wall orientation and shading of the walls was also not investigated. Regulatory requirements, such as the installation of a vapor retarder on the inside surface of the wall, may actually cause harm rather than protect the integrity of the system.

For the code-complying wall system, the wall system took more than 2.5 years to dry out to acceptable levels that would reduce the risk on mold-fungi damage. As a period of only four weeks is sufficient under these environmental conditions to initiate mold growth, this particular EIFS wall would be prone to damage.

The effect of water penetration developed highly localized moisture conditions within the wall, which maintained enough moisture to be prone to moisture damage. The wall system that had a high water penetration due to window interface defects developed a net yearly increase in total moisture when a 6-mil polyethylene vapor retarder was employed. This, however, was not observed for the same high water penetration wall case that did not employ a 6-mil polyethylene vapor retarder. In this case, the wall had the capability to dry toward the interior.

In summary, the following can be concluded:

- To properly model the hygrothermal performance of EIFS walls requires at least a two-dimensional heat, air, and moisture transport model. (An extensive analysis comparing one-dimensional and two-dimensional results is not presented in this paper.)
- Polyethylene vapor retarders and interior paint coatings affect the hygrothermal performance of EIFS wall systems. Substantially slower drying rates for the south-facing EIFS walls were found when vapor retarders were used in climates such as Wilmington.
- Solid south-oriented EIFS walls, i.e., walls with no water penetration from defects, dry out for the climatic conditions found in Wilmington, with a strong dependence on the interior wall permeance conditions.
- High relative humidities were found to persist in the OSB when water penetration defects around windows were included in the simulations.
- The hygrothermal performance of the EIFS walls depends on the amount of water penetration. The characterization of water leakage performance must be better understood for a wider range of pressure differences and water application rates. Wood decay can occur when high relative humidities and moderately high temperature (70% or 80% RH and above 5°C) conditions exist. The likelihood for these to occur in Wilmington is quite high due to the low potential for drying (environmental factor) and the high relative humidities predicted under the window area. Future laboratory measurements should focus on determining the water entry rates into the wall systems.
- With high water penetration rates and low vapor permeance on the interior, moisture accumulated in the wall; with low water penetration rates or high vapor permeance on the interior, moisture did not produce a net yearly accumulation in the wall.

The results provided in this paper are only applicable to the specific materials, wall specifications, and weather condi-

tions employed. Further work is needed to characterize the effects of defects in the exterior surface or possible moisture infiltration or exfiltration from the interior or exterior environments.

Today, by effectively employing advanced moisture engineering analysis and integrating material properties, system and subsystem performances (lab and field studies) and modeling building envelope systems can be optimally designed and assessed for long-term performance. Advanced hygrothermal modeling is an efficient means to develop engineered construction products, similar to other high-tech industries such as aerodynamics, automotive, and even the electronic fields.

ACKNOWLEDGMENTS

The authors of this study would like to thank Mr. John Lackey and Mr. Marchand, technical officers at National Research Canada, for his assistance in the measurements and sample preparation. The Joint Research Project funding by the USG Corporation is gratefully acknowledged (Dr. Tonyan). The technical discussions with Mr. Brown, Dr. Kumaran, Mr. Ulett, Mr. Salonvaara, and other NRC staff are gratefully acknowledged.

REFERENCES

- ASC. 1993. Theory documentation for TASCflow, Version 2.2. Advanced Scientific Computing Ltd., Waterloo, Ontario, Canada.
- ASHRAE. 1997. *1997 ASHRAE Handbook—Fundamentals*. Atlanta: American Society of Heating, Refrigerating and Air-Conditioning Engineers, Inc.
- Bomberg, M., J. Lstiburek, and F. Nabhan. 1997. Performance evaluation of exterior insulation and finish systems (EIFS). Seventh Conference on Building and Science and Technology, March 20-21, pp.1-15.
- Brown, W., J. Ulett, A. Karagiozis, and T. Tonyan. 1997. Barrier EIFS clad walls: Results from a moisture engineering study. *J. Thermal Insul. and Bldg. Envs.*, Vol. 20 (Jan.):. 1-21.
- Choi, E.C.C. 1992. Simulation of wind-driven-rain around a building. *Journal of Wind Engineering*, 52: 60-65.
- Choi, E.C.C. 1991. Numerical simulation of wind-driven rain falling onto a 2-D building. In *Computational Mechanics*, ed. by Cheung, Lee, and Leung, pp.1721-1727. Rotterdam: Balkema.
- Crandell, J.C., and T. Kenny. 1995. Investigation of moisture damage in single-family detached houses sided with exterior insulation finish systems in Wilmington, NC. NAHB Research Center, Inc., August
- EIMA. 1997. EIMA (Exterior Insulation and Finish System [EIFS] Industry Members Association), private communication.
- Hens, H., and A. Janssens. 1993. Inquiry on HAMCAT CODES. International Energy Agency, Heat, Air and Moisture Transfer in Insulated Envelope Parts, Report Annex 24, Task 1, Modeling.
- Karagiozis A. 1997a. Porous media transport in building systems. CFD Society of Canada, Victoria, May 25-27, pp. 7-21 to 7-25.
- Karagiozis A. 1997b. *Moisture Engineering, Proceedings Seventh Conference on Building Science and Technology, Toronto, March 20-21*, pp. 93-112.
- Karagiozis, A., G. Hadyisophocleous, and S. Cao. 1997. Wind-driven rain distributions on two buildings. *Journal of Wind Engineering and Industrial Aerodynamics*, Vols. 67 and 68, pp. 559-572.
- Karagiozis, A., and G. Hadjisophocleous. 1995. Wind-driven rain on high-rise buildings. *Thermal Performance of Exterior Envelopes of Buildings VI*. Atlanta: American Society of Heating, Refrigerating and Air-Conditioning Engineers, Inc.
- Karagiozis, A., M. Salonvaara, and K. Kumaran. 1994. LATENITE hygrothermal material property database. IEA Annex 24 Report T1-CA-94/04, Trondheim, Norway.
- Karagiozis, A. 1993. Overview of the 2-D hygrothermal heat-moisture transport model LATENITE. Internal IRC/BPL Report.
- Kumaran, M.K., G.P. Mitalas, R. Kohonen, and T. Ojanen. 1989. Moisture transport coefficient of pine from gamma ray absorption measurements. *ASME HTD*, Vol. 123, pp. 179-183.
- Lackey, J.C., R.G. Marchand, and M.K. Kumaran. 1997. A logical extension of the ASTM Standard E96 to determine the dependence of water vapor transmission on relative humidity. *ASTM STP 1320*, pp. 456-468.
- Lacy, R.E. 1965. Driving-rain maps on the onslaught of rain on buildings. Current Paper No. 54, Building Research Station, Garston, U.K.
- Lacy, R.E. 1951. Distribution of rainfall round a House. *Meteorol. Magazine*, 80 (1951): 184-189.
- NCDC. 1995. Weather data for Wilmington, N.C. Natural Resource Center, National Climatic Data Center.
- Nelson, P., and M. Waltz. 1996. EIFS—Surface sealed wall systems that need flashings. *Exterior insulation finish systems (EIFS): Materials, properties, and performance, ASTM STP 1269*, pp. 149-164.
- Nisson, N.J.D. 1995. Severe rotting found in homes with exterior insulation systems. *Energy Design Update*, 15, No. 12 (Dec.), pp.1-3.
- Posey, B.J., and J. Vlooswyk. 1996. *EIFS: Canadian field performance, exterior insulation finish systems (EIFS): Materials, properties, and performance, ASTM STP 1269*, pp. 3-20. American Society for Testing and Materials.
- Salonvaara, M., and A. Karagiozis. 1994. Moisture transport in building envelopes using an approximate factorization solution method. CFD Society of Canada, Toronto, June 1-3.

- Schwarz, B., and W. Schlagregen. 1973. *Berichte aus der Bauforschung*, Heft 86, Berlin 1973.
- Ullett, J. 1996. NRC Client Report pn: Exterior Insulation Systems Water Penetration Study Task 2a, Evaluate and Characterize Water Penetration into the EIFS systems Based on Full Scale Test Results.
- USG Corporation Client Report. 1996. Exterior insulation finish system water penetration study. National Research Council Canada by W.C. Brown, J. Ullett, A.N. Karagiozis, and K. Kumaran.
- Wisse, J.A. 1994. Driving rain, A numerical study. 9th Symposium for Building Physics and Building Climatology, 14-16 Sept. 1994, Dresden.
- Zwayer, G. 1996. EIFS: When It works, when it does not. *Exterior insulation finish systems (EIFS): Materials, properties, and performance, ASTM STP 1269*, pp. 21-25. American Society for Testing and Materials.